Journal of Environmental Management 354 (2024) 120345

Contents lists available at ScienceDirect

Journal of Environmental Management

journal homepage: www.elsevier.com/locate/jenvman

Research article

Reducing biosolids from a membrane bioreactor system: Assessing the effects on carbon and nutrient removal, membrane fouling and greenhouse gas emissions

Paulo Marcelo Bosco Mofatto, Alida Cosenza, Daniele Di Trapani, Giorgio Mannina *

Engineering Department, Palermo University, Viale delle Scienze, Bdg. 8, 90128, Palermo, Italy

ARTICLE INFO

Handling Editor: Prof Raf Dewil

Keywords:
Carbon footprint
Circular economy
Wastewater treatment
Biosolid management

ABSTRACT

This study presents the effects on carbon and nutrient removal, membrane fouling and greenhouse gas (GHG) emissions of an Oxic-Settling-Anaerobic (OSA) – Membrane Bioreactor (MBR) pilot plant fed with real wastewater. The influence of three sludge return internal ratios (IR) was investigated by testing 45, 75 and 100%. The results showed that with the increase of IR, the biological sludge production substantially decreased by 85.8% due to the combination of cell lysis and endogenous metabolism. However, a worsening of ammonia removal efficiencies occurred (from 94.5 % to 84.7 with an IR value of 45 and 100%, respectively) mostly due to the ammonia release caused by cell lysis under anaerobic conditions. The N_2O emission factor increased with the rise of IR (namely, from 2.17% to 2.54% of the total influent nitrogen). In addition, a variation of carbon footprint (CF) (0.78, 0.62 and 0.75 $kgCO_{2eq}$ m^{-3} with 45, 75 and 100% IR, respectively) occurred with IR mainly due to the different energy consumption and carbon oxidation during the three periods. The study's relevance is to address the optimal operating conditions in view of reducing sludge production. In this light, the need to identify a trade-off between the advantages of reducing sludge production and the disadvantages of increasing membrane fouling and GHG emissions must be identified in the future.

1. Introduction

There is a great concern regarding the production of excess sewage sludge (Mannina et al., 2023a,b). In 2020, in Europe, about 13 million tons of dry matter of biological sewage sludge were produced by urban wastewater treatment plants (WWTPs) (Collivignarelli et al., 2021). Since the management and disposal of excess sludge can strongly contribute to the total plant operational costs (up to 60%) (Etienne and Yu-Tung, 2012). In this regard, efforts have been made in the scientific and industrial community to study and identify processes and technologies that can reduce sewage sludge production in WWTPs. Several technologies have been proposed to minimise excess sludge production based on chemical, physical, thermal and biological processes (Zhang et al., 2021a,b). The last represents the most interesting from an environmental point of view because they are more sustainable than chemical processes (Collivignarelli et al., 2021). Among biological processes, the oxic-settling-anaerobic (OSA) process represents a promising alternative (Morello et al., 2021). This process configuration is based on a modification of the conventional activated sludge (CAS) layout by placing an anaerobic reactor in the return activated sludge (RAS) line (Chudoba et al., 1992). In this reactor, the sludge is subjected to conditions with low oxygen and substrate, and then it is recirculated to the main reactor (Semblante et al., 2014). Excess sludge reduction in the OSA process occurs through different mechanisms, including uncoupled metabolism, biomass decay, extracellular polymeric substances (EPS) destruction, bacterial predation, and selection of slow-growing bacteria (Ferrentino et al., 2021). Compared to other technologies, the OSA process is readily applied to existing CAS plants without requiring any physical or chemical pre-treatment (Semblante et al., 2014). Literature suggests that depending on the return internal ratio (IR) from the settler to the anaerobic reactor, the reduction of sewage sludge production compared to CAS can vary from 10% to 60% with strong implications in terms of operational cost reduction (among others, Romero-Pareja et al., 2017; Ferrentino et al., 2021). According to the literature, an effective sludge yield reduction can be achieved by combining the OSA system with a membrane biological reactor (MBR) (Fida et al., 2021). The typical operational conditions of MBR (e.g., high sludge retention time) can favour some mechanisms such as uncoupled

* Corresponding author.
E-mail address: giorgio.mannina@unipa.it (G. Mannina).

https://doi.org/10.1016/j.jenvman.2024.120345
Received 9 October 2023; Received in revised form 12 January 2024; Accepted 8 February 2024
Available online 23 February 2024

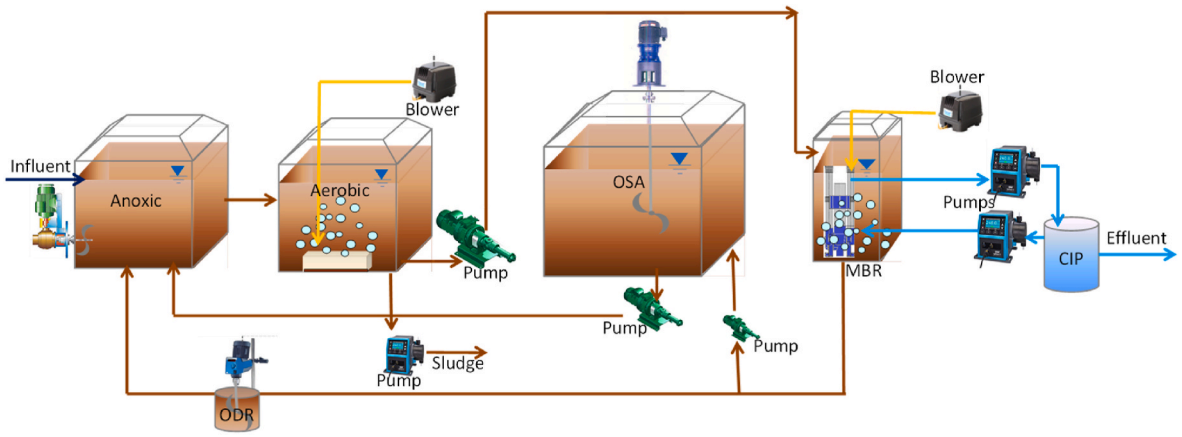

Fig. 1. Schematic layout of OSA-MBR system.

metabolism, biomass decay, and selection of slow-growing bacteria (Semblante et al., 2014, 2016; Fida et al., 2021). Indeed, the application of the OSA process using MBR reported in the literature suggests excellent results in terms of sewage sludge reduction with a reduction of up to 40% (Cosenza et al., 2023; Mannina et al., 2023a,b). From a practical point of view, integrating an OSA configuration with an existing MBR system could represent an easy solution for plant operators in view of further decreasing the excess sludge production. However, some relevant operational aspects have been neglected in previous studies applying the OSA process with MBR. For example, two critical elements, such as the influence on greenhouse gas (GHG) emissions and the consequent effect on the plant carbon footprint (CF) have been neglected (Culaba et al., 2022). A literature study showed a reduction of GHG emissions of around 23% than CAS but without MBR (Liu et al., 2021). Despite OSA's potential beneficial role, previous literature studies were obtained by applying life cycle assessment analysis based on emission factors without any measured data. As far as the authors are aware, no studies exist on assessing plant performances in pollutant removal and greenhouse gas emissions for OSA-MBR treating real wastewater, emphasising the attention on CF. Moreover, since membrane fouling still represents a critical issue of MBR systems (Zhang and Jiang, 2019; Chen et al., 2019; Zhang et al., 2021a,b; 2022), the assessment of the relationship between fouling tendency IR to the anaerobic reactor in an OSA-MBR process is pivotal. In light of the above, the paper presents a comprehensive study to assess the effects of three different IRs on pollutant removals, membrane fouling and greenhouse gas emissions for an OSA-MBR pilot plant fed with real wastewater.

2. Material and methods

2.1. Pilot plant configuration

An MBR pilot plant was built at the Water Resource Recovery Facility of Palermo University (Mannina et al., 2021a, 2021b) and was fed with real wastewater. Using a pre-denitrification scheme, the OSA-MBR configuration was conceived for carbon and nitrogen removal (Fig. 1). Therefore, the pilot plant was characterised by the following units: one anoxic reactor (V = 110 L) and one aerobic reactor (V = 240 L), followed by a membrane bioreactor (V = 48 L) with an ultrafiltration hollow fibre membrane module (Fig. 1) (hollow fibre porosity of 0.03 μm and membrane surface of 1.4 m^2). The membrane reactor had a clean-in-place (CIP) system for ordinary backwashing.

An oxygen depletion reactor (ODR) (V = 53 L) was inserted in the internal recycling line between the aerobic and anoxic reactors in view of depleting the dissolved oxygen concentration before entering the anoxic reactor. To realise the OSA configuration, an anaerobic side-stream reactor (ASSR) (V = 275 L) was inserted in the RAS line.

2.2. The experimental campaign and analytical methods

The experimental campaign was divided into periods: Period I, II, and III. All periods were operated according to OSA-MBR configuration (with HRT = 6 h) but changing the IR of the MBR reactor to OSA tank: 45%, 75% and 100% in Periods I, II and III, respectively.

The operational parameters, such as DO, pH and oxidation-reduction potential (ORP), were monitored daily using specific probes connected to a multimeter (WTW 3340). Other parameters, such as chemical oxygen demand (COD), ammonia nitrogen (NH_4^+-N), nitrate (NO_3^-N), nitrite (NO_2^-N), orthophosphate (PO_4^{3-}P), total suspended solid (TSS) and volatile suspended solid (VSS) concentrations, biological oxygen demand (BOD) and Total Nitrogen (TN) were measured twice a week

Table 1
Average values of the main influent and operational features for each experimental Period; SD = Standard Deviation.

Parameter	Symbol	Units	Period I IR = 45%		Period II IR = 75%		Period III IR = 100%	
			Average	SD	Average	SD	Average	SD
Total COD	TCOD	[mg L^{-1}]	1152	207	1210	431	1187	220
Soluble COD	sCOD	[mg L^{-1}]	142	46	184	53	229	71
Total Nitrogen	TN	[mg L^{-1}]	38	6	32	2	28	3
Ammonium	NH_4–N	[mg L^{-1}]	25	4	31	9	27	4
Phosphate	PO_4–P	[mg L^{-1}]	9	3	13	6	7	3
Flow Rate	Q_{IN}	[L h^{-1}]	17.9	2	16.6	2	18.2	2
Food/Microorganism Ratio	F/M	[gCOD/gTSS d]	0.23	0.14	0.30	0.05	0.23	0.14
Sludge Retention Time	SRT	[d]	53	18	65	6	65	5

according to Standard Methods (APHA, 2012). Respirometric tests have been performed once per week to analyse the kinetic parameters, according to Di Trapani et al. (2014). The sludge volume index (SVI) was evaluated in the aerobic mixed liquor once a week. Furthermore, extracellular polymeric substances (EPS) and soluble microbial products (SMP), both in terms of carbohydrates and proteins, have been analysed according to literature (Mannina et al., 2017) one time per week in the mixed liquor of anoxic, aerobic, ASSR and MBR tanks. According to Mannina et al. (2017), total EPS were the sum between bound EPS and SMP as carbohydrates and proteins (EPS_p, EPS_c, SMP_p, SMP_c). Nitrous oxide (N_2O–N) concentration in the liquid and gaseous phase of all the reactors has been measured two times per week by using a gas chromatograph equipped with an Electron Capture Detector (ECD) according to Mannina et al. (2016a,b). Moreover, the N_2O–N fluxes have also been quantified using each reactor's off-gas flow rate measurement.

2.3. Wastewater features and operation

The experimental campaign was divided into three Periods. Table 1 summarises the average and standard deviation (SD) quality and quantity features of the influent wastewater and the plant operational conditions (regarding sludge retention time – SRT and Food/Microorganism Ratio – F/M) for each experimental Period.

2.4. Excess sludge production quantification

The sludge reduction was calculated by the reduction of biological sludge production calculated in the three periods. The biological sludge was calculated as the difference between the total sludge production (Tsludge) and the primary sludge (Psludge), according to Mannina et al. (2022). The TSS concentrations in the reactors were kept almost constant between the different periods.

The observed yield coefficient (Y_{obs}) was calculated as the ratio between the cumulative mass of TSS produced and the cumulative mass of COD removed, according to literature (Mannina et al., 2002) (eq. (1)).

$$Y_{obs} = \frac{\Delta X}{Q_i \bullet (TCOD_{in} - TCOD_{out})} \left(gSST\ gCOD^{-1}\right) \quad \text{(eq 1)}$$

$TCOD_{in}$ and $TCOD_{out}$ are concentrations in the influent and effluent, respectively. Qi is the daily influent flow rate, and ΔX is the daily excess sludge production.

2.5. Membrane fouling

Membrane fouling was quantified by monitoring the transmembrane pressure (TMP) (kPa) and the permeate flux (J) ($m^3\ m^{-2}\ s^{-1}$) every day to calculate the total membrane resistance (R_T) to filtration, according to Equation (2).

$$R_T = \frac{\Delta P}{\mu \bullet J} \left(m^{-1}\right) \quad \text{(eq 2)}$$

where ΔP [kPa] is the TMP variation and μ [Pa s] is the permeate viscosity.

A resistance in series (RIS) model was applied according to the literature (Di Bella et al., 2018) (Equation (3)).

$$R_T = R_m + R_C + R_P \left(m^{-1}\right) \quad \text{(eq 3)}$$

where R_m, R_C and R_P represent respectively the intrinsic resistance due to the clean membrane, the resistance due to the cake layer and the resistance due to the pore fouling.

Membrane fouling was controlled by performing physical and chemical cleanings. Physical and chemical cleanings required the membrane to get off from the MBR tank. Physical cleaning was done by manually removing the solids from the membrane surface and flushing with clean water. After each physical cleaning, the membrane was submerged into a tank with clean water, and the total resistance after membrane cleaning (R_{T1}) was measured according to Equation (2). Since the cake layer was removed, R_{T1} represented the sum between R_m and R_P. Therefore, the RP was obtained by subtracting from R_{T1} the R_m value. Subsequently, the membrane was submerged into the mixed liquor, and the total resistance after the first cycle was acquired (R_{T2}) according to Equation (2). Consequently, according to Equation (3) the R_C value was evaluated as in Equation (4).

$$R_C = R_{T2} - R_m - R_P \left(m^{-1}\right) \quad \text{(eq 4)}$$

Chemical cleanings were performed by using a 4% sodium hypochlorite solution according to the manufacturer's suggestion.

2.6. Greenhouse gas measurement, carbon footprint and effluent quality calculation

N_2O–N concentration was measured both in the liquid and in the gaseous phase. The sampling procedure described by Mannina et al. (2018) was adopted. N_2O–N concentration was analysed by using a Gas Chromatograph (GC) (Thermo Scientific™ TRACE GC) equipped with an Electron Capture Detector (ECD).

In view of evaluating the amount of influent nitrogen converted into N_2O–N, the N_2O–N emission factor (EF_{N2O}) was quantified according to the literature (Tsuneda et al., 2005; Mannina et al., 2016a,b).

CF has been quantified as the sum of three contributions: direct, indirect and derived emissions. Direct emissions (DE) refer to the amount of CO_2 directly related to the organic carbon oxidation ($CO_{2,OrgOx}$), endogenous respiration ($CO_{2,Endog.}$) and N_2O emission ($CO_{2eq,N2O}$). This latter has been quantified as equivalent CO_2 by multiplying the N_2O emission by its global warming potential (GWP). $CO_{2,OrgOx}$, $CO_{2,Endog}$ have been quantified according to Boiocchi et al. (2023).

In view of quantifying CO_{2eq} the measured data have been used (Equation (5)).

$$CO_{2,N2O} = Q_g \bullet C_{g,N2O} \bullet GWP_{N2O} \left(kgCO_{2eq}\ /\ d\right) \quad \text{(eq 5)}$$

where Q_g [m^3/d] is the average gas flow, Cg,N2O [kgN_2O/m^3] is the average gaseous measured N_2O concentration emitted and GWPN2O [$kgCO_{2eq}/kgN_2O$] is the N_2O global warming potential, equal to 298 according to IPCC (2022).

Indirect emissions (IE) are due to the CO_2 generated from energy consumption ($CO_{2eq,En}$) and sludge management (treatment, transportation and disposal) ($CO_{2eq,Sludge}$). This latter has been quantified according to Equation (6).

$$CO_{2eq,Sludge} = M_{sludge} \bullet FC_{Sludge} \left(kgCO_{2eq}\ /\ d\right) \quad \text{(eq 6)}$$

where M_{sludge} [ton/day] is the mass of wasted sludge per day and FCSludge [$kgCO_{2eq}$/ton] is the emission factor due to the sludge management (equal to 714.74 $kgCO_{2eq}$/ton according to Zhao et al. (2023)).

Derivative emissions (DerE) have been quantified as originating from the pollutants discharged into receiving water bodies (Equation (7)).

$$DerE = CO_{2eq,effBOD} + CO_{2eq,effN2O} \left[kgCO_{2eq}\ /\ d\right] \quad \text{(eq 7)}$$

Each contribution of Equation (7) has been quantified according to Boiocchi et al. (2023), considering the N_2O measured data of the treated effluent.

The effluent quality index (EQI) expressed as the mass of pollutant (PU) discharged daily has been calculated according to Equation (8).

$$EQI = \frac{1}{T \bullet 1000} \bullet \int_{t_0}^{t_1} (\beta_{COD} \bullet TCOD + \beta_{TN} \bullet TN + \beta_{PO} \bullet PO_4 - P) \bullet Q_{out} \bullet dt \quad \text{(eq 8)}$$

where β_{COD}, β_{TN} and β_{PO} represent the weighting factor of the effluent concentration of TCOD, TN and PO_4–P, respectively. The 1, 20 and 50

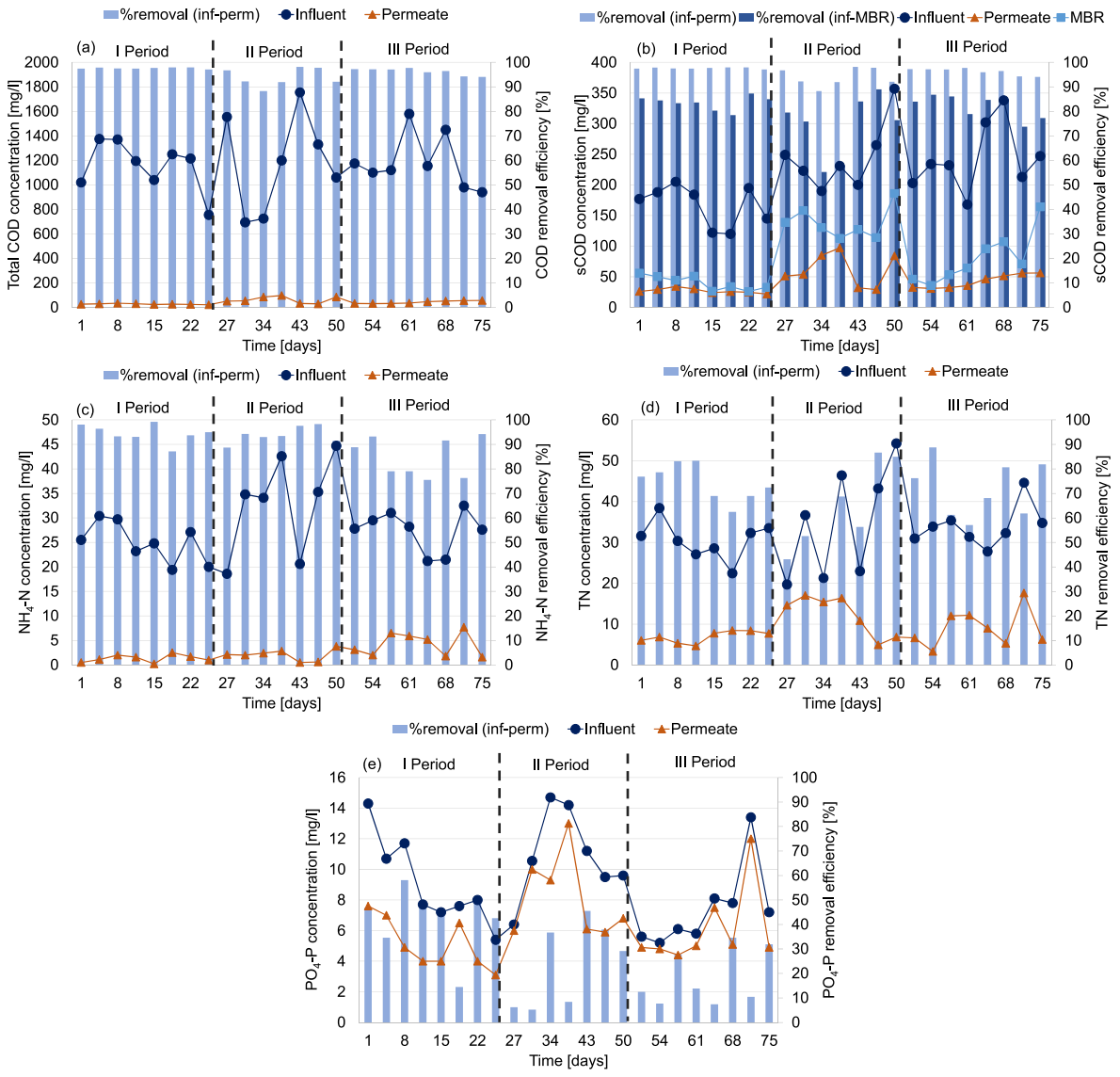

Fig. 2. Influent and effluent concentrations, as well as the removal efficiencies during experiments of TCOD (a), sCOD (b), ammonia (c), TN (d) and phosphorus I.

values have been adopted here for β_{COD}, β_{TN} and β_{PO} (Mannina and Cosenza, 2015).

3. Results and discussion

3.1. Pilot plant performance

Fig. 2 shows the pilot plant performance results obtained for each experimental Period regarding TCOD, sCOD, NH_4–N, TN and PO_4–P removal. Regarding the TCOD, the results showed that despite the influent variability, the IR increasing from Period I to Period III did not affect the removal efficiency (Fig. 2a). Indeed, the average TCOD removal efficiency was equal to 97.6% (±0.3), 94% (±3.5) and 96.3% (±1.4) for Period I, Period II and Period II, respectively. This result was mainly attributed to the capability of the membrane to retain all the substances having an average diameter higher than 0.03 μm. This result seems to align with previous literature, which suggested that the increase of IR from 0 to 22% does not compromise the effluent quality in an MBR system (Fida et al., 2021). However, in this study, different to the existing literature, a detailed analysis was performed, discriminating IR's effect on the biological and physical COD removal. Indeed, Fig. 2b shows the trend of influent and effluent sCOD profile concentration.

Further, in Fig. 2b, the trend of the sCOD profile concentration inside the MBR tank (before filtration) is also shown. Using the sCOD concentration inside the MBR, it was possible to discriminate between the biological and physical removal of sCOD. Data revealed that the biological removal of sCOD was influenced by the increase of IR from Period I to Period II (Fig. 2b). Indeed, the average sCOD removal efficiency was equal to 76% (±5), 43% (±10) and 67% (±15) for Period I, Period II and Period III, respectively. This result was likely debited to cell lysis due to the increase of IR, which increased the amount of sCOD to be removed, thus reducing the sCOD removal efficiency with the IR increase. This result was evident in terms of NH_4–N. As shown in Fig. 2c, the IR increase influenced nitrification efficiency. Indeed, the average nitrification efficiency decreased from 95.5% (±3.8) for Period I to 85.7% (±8) for Period III (average value of 94% ± 3.3 for Period II). The decrease in nitrification efficiency could be attributed to the ammonia release due to the cell lysis and to the inability of the autotrophic bacteria to oxidise all the available ammonia. Indeed, as discussed in the respirometry section, autotrophic biomass was not particularly stressed by the increase in IR value. Similar results were obtained in a previous study (Fida et al., 2021). The decrease of the ammonia oxidation led to the consequent decrease of TN removal with the IR increasing. Indeed, the average TN removal efficiency decreased from 74% to 61% from

Table 2
Observed biomass yield coefficient at the environment temperature ($Y_{obs,T}$) and corrected at 20 °C ($Y_{obs,20}$) and percentage of biological sludge reduction for experimental Periods I, II and III.

	Period		
	I	II	III
$Y_{obs,T}$ [gTSS/gCOD]	0.2	0.14	0.12
$Y_{obs,20}$ [gTSS/gCOD]	0.25	0.20	0.15
T [°C]	28.6	27.9	28.2
Biological sludge reduction [%]	–	86	88
Cumulative TSludge [gTSS]	673	46.3	45.7
Cumulative PSludge [gTSS]	482	8	13

Period I to Period III. Regarding the PO_4–P (Fig. 2e), the removal efficiency strongly decreased with the IR increase. Indeed, the average PO_4–P removal efficiency was 42% (±13) for Period I, 24.2 % (±10) for Period II and 18.3% (±11) for Period III. According to the literature, this result could be related to PO_4–P release inside the OSA reactor and the nutrient release due to the cell lysis (Semblante et al., 2016). Indeed, sporadic measurements of PO_4–P inside the anoxic reactor revealed an increase of 20%, 28%, and 35% compared to the influent concentration.

3.2. Sludge reduction

In Fig. S1 (Supplementary Information) the trend of TSS and VSS concentrations measured over the three experimental periods in the influent wastewater and inside all the reactors are reported. The average TSS concentration of the influent wastewater was 536 mg L^{-1}, 520 mg L^{-1} and 670 mg L^{-1} for Period I, II and III, respectively. The average TSS/VSS in the influent wastewater was 65% for Periods I and II and 50% for Period III. The fluctuations of influent TSS concentration influenced its concentration inside the reactors. In particular, the decrease of TSS concentration in the influent wastewater during the first days of Period II influenced the TSS concentration inside all the reactors, which slightly decreased. The average TSS concentration was maintained in the anoxic reactor at around 2800 mg L^{-1} $^{on\ average}$. In the aerobic reactor, the TSS concentration was around 3000 mg L^{-1} (Fig. S1c). While inside the ASSR and MBR compartments, the average TSS concentration was maintained at approximately 3500 mg L^{-1} (Figs. S1d–e). It was noted that the average VSS/TSS ratio decreased with the increase in IR in all the reactors (Fig. S1). In the anoxic reactor, the VSS/TSS ratio decreased from 89% (Period I) to 74% (Period III) (with a value of 79% during Period II) (Fig. S1b). In the aerobic reactor, the VSS/TSS ratio decreased from 85% (Period I) to 75% (Period III) (with a value of 78% during Period II) (Figure SI1c). At the same time, a very similar reduction of VSS/TSS occurred in ASSR and MBR reactors with average values of around 85% (Period I), 80% (Period II) and 75% (Period III) (Figs. S1d–e). The volatile destruction obtained in all the reactors with the IR increase indicates cell lysis, thus justifying the nutrient release discussed above. This result agrees with previous literature. For example, Fida et al. (2021) obtained a VSS/TSS reduction inside the anoxic reactor of an MBR system aimed at nutrient removal. Semblante et al. (2016) tested the effect of IR in a sequential batch reactor (SBR) OSA system and found that the IR increase led to cell lysis and the decrease of VSS/TSS, especially inside the anoxic reactor. However, unlike the previous literature, the results obtained here show a reduction of the VSS/TSS ratio inside all the reactors. This was mainly debited to the high SRT values over the three experimental periods (53 days – Period I and 65 days – Periods II and III) favouring the endogenous metabolism and the consequent VSS reduction (Metcalf, 2015).

Table 2 summarises the observed biomass yield coefficient at the environment temperature ($Y_{obs,T}$) and 20 °C ($Y_{obs,20}$), the percentage of biological sludge reduction, and the cumulative TSludge and PSludge for each experimental Period. It was noticed that the higher the IR value, the lower the total and biological excess sludge production was (Table 2). In comparison with Period I (OSA-MBR, IR = 45%), Period III (OSA-MBR, IR = 100%) showed a reduction of 88% in biological excess sludge production (Table 2). This result was also confirmed by the decrease of the average Y_{obs} from Period I to II and III (0.20, 0.14 and 0.12 gTSS/gCOD, respectively) (Table 2).

Despite the variability of the influent wastewater quality, the results obtained here regarding biomass yield coefficient are almost in line with those obtained in literature studies carried out with synthetic wastewater. For example, Ferrentino et al. (2018), under 100% IR, obtained a Y_{obs} value of 0.12 g TSS $gCOD^{-1}$. However, Ferrentino et al. (2018) obtained a lower sludge reduction, accounting for 66% when the IR was increased; this result was likely related to the higher SRT established.

3.3. Sludge properties

To evaluate the effect of IR on the sludge properties, the bound EPS (both as carbohydrates and proteins – EPS_c and EPS_p) and SMP (both as carbohydrates and proteins – SMP_c and SMP_p) were measured in the mixed liquor of all the reactors coupled with the SVI, evaluated in the aerobic mixed liquor. In Table 3 the average and standard deviation data of EPS, SMP and SVI are reported.

The IR did not influence the average SVI value. Indeed, the average SVI value was equal to 153 mL $gTSS^{-1}$ – Period I, 120 mL $gTSS^{-1}$ – Period II and 138 mL $gTSS^{-1}$ – Period III. The high SVI values obtained during all the experimental periods were likely due to the high SRT value, which could have promoted the growth of filamentous bacteria, as highlighted by Zhang et al. (2019).

In terms of EPS, a progressive reduction of the total EPS with the IR increasing occurred, as average. Specifically, the total amount of EPS in

Table 3
Specific average and SD concentration of each EPS fraction and SVI for each reactor and experimental Period.

Period		SMP_P		SMP_C		EPS_P		EPS_C		SVI	
		mg $gTSS^{-1}$		mg $gTSS^{-1}$		mg $gTSS^{-1}$		mg $gTSS^{-1}$		mL$gTSS^{-2}$	
		Mean	SD	Mean	SD	Mean	SD	Mean	SD	Mean	SD
I	Anoxic	1.04	0.85	1.65	1.06	82.85	25.66	6.37	1.46	–	–
	Aerobic	1.76	1.55	3.66	2.33	79.66	33.98	6.13	1.63	153	40
	OSA	0	0	0.87	0.35	76.05	20.26	5.36	1.04	–	–
	MBR	0	0	1.74	0.69	74	23.02	6.14	1.74	–	–
II	Anoxic	31.61	7.79	6.19	2.52	54.2	1.25	0	0	–	–
	Aerobic	57.13	6.36	8.1	6.86	43.3	25.2	0	0	120	14
	OSA	7.24	5.25	8.07	2.2	59.67	12.2	0.01	0.02	–	–
	MBR	13.55	10.09	9.49	9.19	25.9	4.98	4.35	6.15	–	–
III	Anoxic	7.73	8.99	4.17	5.89	48.88	4.42	9.26	10.26	–	–
	Aerobic	3.16	1.03	3.71	4.32	47.43	8.23	9.03	10.61	138	18
	OSA	8.04	7.78	1.67	0.53	27.28	2.66	6.66	4.98	–	–
	MBR	14.59	3.93	12.58	2.59	30.98	6.27	4.42	4.12	–	–

Table 4
Summary of the main heterotrophic and autotrophic kinetic and stoichiometric parameters as average values (in brackets the standard deviation).

Parameter	Symbol	Units	Heterotrophic		
			IR 45%	IR 75%	IR 100%
			OSA-MBR	OSA-MBR	OSA-MBR
Max. growth yield	Y_H	[gVSS g^{-1}COD]	0.39 (±0.04)	0.38 (±0.06)	0.35 (±0.02)
Decay rate	b_H	[d^{-1}]	0.80 (±0.05)	0.68 (±0.21)	0.59 (±0.04)
Max. growth rate	μ_H	[d^{-1}]	2.54 (±0.42)	1.20 (±0.34)	1.28 (±0.87)
Max. removal rate	ν_H	[d^{-1}]	7.33 (±1.87)	3.14 (±0.46)	3.77 (±2.72)
Net growth rate	μ_H- b_H	[d^{-1}]	1.96 (±0.39)	0.52 (±0.43)	0.69 (±0.91)
Active fraction	f_X	[%]	25.10 (±7.42)	19.40 (±4.35)	23.49 (±6.05)
Parameter	**Symbol**	**Units**	**Autotrophic**		
			IR 45%	**IR 75%**	**IR 100%**
			OSA-MBR	OSA-MBR	OSA-MBR
Max. growth yield	Y_A	[gVSS $g^{-1}NH_4$–N]	0.11 (±0.02)	0.16 (±0.03)	0.21 (±0.03)
Decay rate	b_A	[d^{-1}]	0.12 (±0.01)	0.12 (±0.06)	0.14 (±0.01)
Max. growth rate	μ_A	[d^{-1}]	0.25 (±0.04)	0.21 (±0.03)	0.23 (±0.02)
Max. removal rate	ν_A	[d^{-1}]	2.69 (±0.40)	1.35 (±0.07)	0.87 (±0.31)
Nitrification rate	N_R	[$mgNH_4$ L^{-1} h^{-1}]	5.95 (±0.76)	2.36 (±1.81)	2.06 (±2.76)

all the reactors was equal to 347 mg $gTSS^{-1}$, 329 mg $gTSS^{-1}$ and 240 mg $gTSS^{-1}$ for Period I, Period II and Period III, respectively (average values). This result was mainly related to the reduction of EPS compounds (both EPS_c and EPS_p), thus suggesting that the EPS destruction occurred with the increase of IR (Table 3), likely due to the increase of the amount of biomass staying under anaerobic conditions (Ferrentino et al., 2018). The EPS destruction is also corroborated by the increase of SMP concentration with the IR increase, as demonstrated in literature by Cheng et al. (2021), who obtained an increase in SMP and cell lysis under anaerobic conditions. The total SMP (expressed as the sum of SMP_c and SMP_p) increased on average from 10.72 mg $gTSS^{-1}$ to 56 mg $gTSS^{-1}$ from Period I to Period III.

3.4. Heterotrophic and autotrophic biomass kinetics

Table 4 summarises the average values of the heterotrophic and autotrophic kinetic parameters obtained in the three experimental periods. From the observation of data reported in Table 4, it can be noticed that the heterotrophic biomass yield showed a slight decrease in the experimental periods, from 0.39 gVSS g^{-1}COD to 0.38 and 0.35 gVSS g^{-1}COD in Periods I and III, respectively. This decrease agrees with the observed Y_H values. This result highlighted that increased sludge recirculation through the anaerobic reactor enhanced the decrease in sludge production. Referring to the heterotrophic decay rate, it was observed a decrease in the achieved values in the different experimental periods; this result, coupled with the decrease of EPS content and the simultaneous increase of SMP released in the anaerobic reactor, could suggest that sludge reduction was ascribable to cell lysis and EPS destructuration, while endogenous decay and uncoupled metabolism could be considered secondary. Referring to the heterotrophic growth rate, a significant decrease was observed from Period I (2.54 d^{-1}) to Period II (1.2 d^{-1}). In contrast, from Period II to Period III, it showed a slight increase, related to the fact that when 100% of sludge was recycled to the anaerobic reactor, the actual retention time in this reactor slightly decreased. The removal rate, the net growth rate and the heterotrophic active fraction showed similar behaviour. Regarding autotrophic species, the results of respirometry batch tests highlighted a slight increase in biomass yield from Period I through Periods II and III, thus indicating that the increase of sludge percentage fed to the anaerobic reactor did not exert stress on biomass yield. In contrast, the decay rate remained almost constant in Period I and II, while it showed a slight increase in Period III, when 100% of the sludge was recycled through the anaerobic reactor. Moreover, the maximum autotrophic growth rate decreased from 0.25 d^{-1} to 0.21 d^{-1} in Period I and Period II, respectively, thus highlighting a stress effect on biomass growth rate. Nevertheless, in Period III, the maximum growth rate increased again from 0.21 d^{-1} to 0.23 d^{-1}, suggesting that an acclimation of autotrophic biomass occurred, likely related to the plant operational conditions. The maximum removal rate, as well as the nitrification rate, showed a decreasing trend from Period I to Periods II and III, thus suggesting a general stress effect on nitrifiers species, mainly due to the increased percentage of sludge fed to the anaerobic reactor, even if it was not observed a dramatic stress effect on autotrophic species.

3.5. Membrane fouling

In Fig. 3 the total membrane resistance (R_T) and the results obtained by applying the RIS model (related to the last physical cleaning

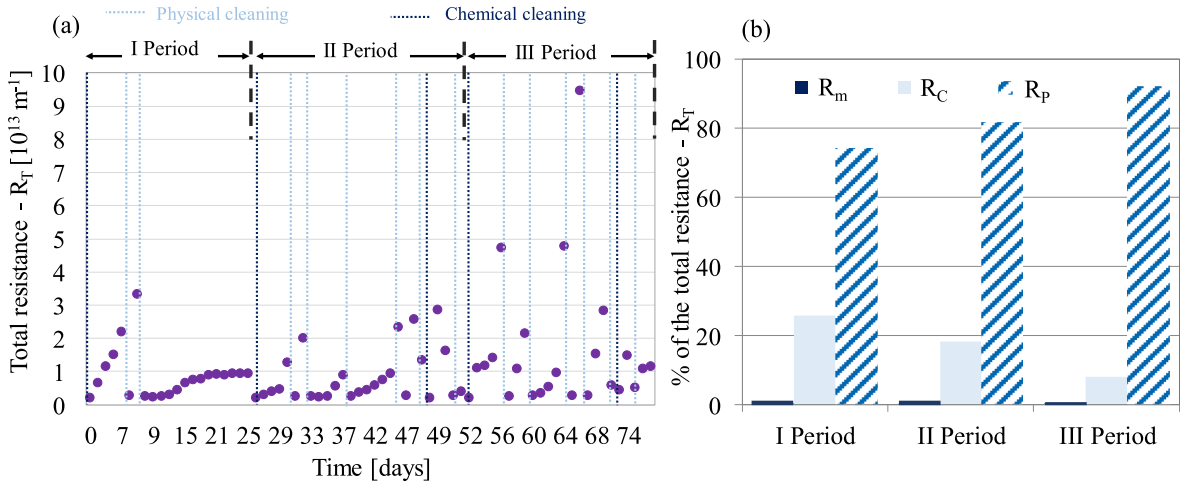

Fig. 3. Total resistance (a) and RIS model application results (b) for each Period.

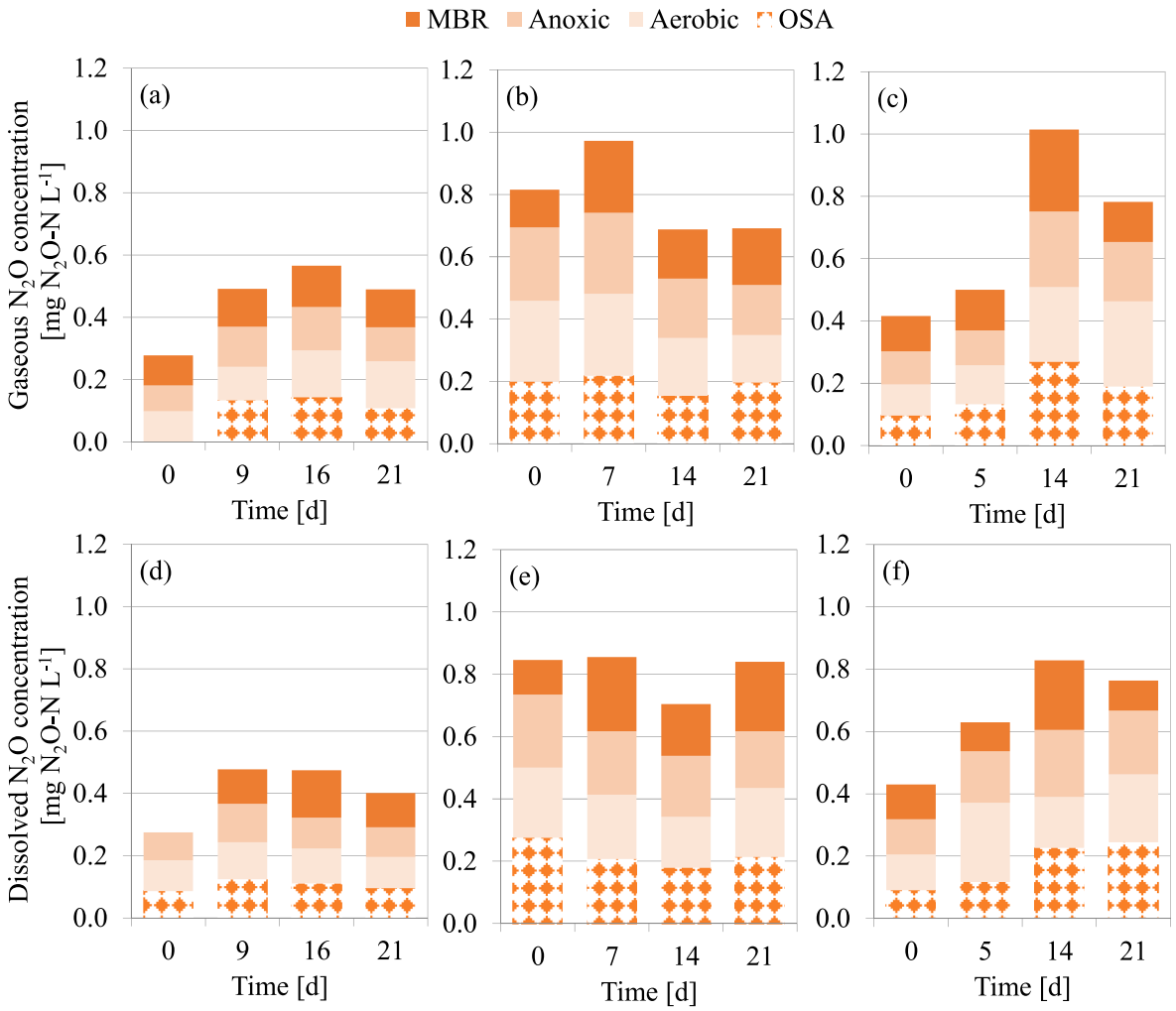

Fig. 4. Gaseous N_2O–N concentration for each reactor in Periods I (a), II (b) and III (c) and dissolved N_2O–N concentration for each reactor in Periods I (d), I(e) and III (f).

performed within each Period) are reported. Results of Fig. 3 show that the IR increase (from 45% to 100%, from Period I to Period III) strongly influenced the membrane fouling. The average R_T value during Period I was 0.82 10^{13} m^{-1} (Fig. 3a). The average R_T value increased to 0.88 10^{13} $m^{-1}$and 1.6 10^{13} m^{-1} during Period II and Period III, respectively. It is worth noting that due to the increase of the membrane fouling with the IR increasing, the amount of physical and chemical cleanings required during the three experimental Periods considerably changed. Specifically, during Period I, only two physical cleanings were required to maintain membrane resistance within the acceptable range suggested by the manufacturer (TMP below 0.7 bar). During Period II, six physical and one chemical cleaning were required. Finally, during Period III seven physical and two chemical cleanings were performed.

The RIS model application confirmed that the IR value increase adversely impacted membrane fouling. Indeed, as shown in Fig. 3b, the amount of resistance due to the pore fouling (R_p) progressively increased (74%, 81%, to 92% for Period I, II and III, respectively) with the increase of IR. This result was mainly debited to the increased SMP favouring irreversible fouling due to their colloidal dimension (Cosenza et al., 2013). The increased amount of membrane cleanings required with increased IR could have important economic implications in the MBR operation. Therefore, a trade-off between the advantages of reducing sludge production and the disadvantages of increasing membrane fouling must be identified. The results obtained here apparently contrast with Fida et al. (2021), who affirmed that the IR value did not affect the membrane resistance. However, the results presented by Fida et al. (2021) revealed an increase in R_T with the increase in IR. The key difference with this study is that Fida et al. (2021) have investigated a different range of IR values (11%, 16.5 and 22%).

3.6. Greenhouse gases

Fig. 4 reports the gaseous and dissolved N_2O–N concentration results for each reactor during Periods I, II and III. Data from Fig. 4 shows that the highest gaseous N_2O–N concentration measured in the headspace of the different reactors occurred in the aerated reactors (aerobic and MBR) for each Period. The average values of the N_2O–N concentration in the aerobic off-gas were 0.12, 0.18 and 0.21 mg N_2O–N L^{-1} in Period I, II and II, respectively. In contrast, for the MBR compartment, the average N_2O–N concentrations in the off-gas were 0.12, 0.16 and 0.17 mg N_2O–N L^{-1} in Periods I, II and II, respectively. This result suggests that the role of the nitrification process in N_2O–N emission is crucial. Indeed, three main N_2O–N production pathways have been identified in the literature: hydroxylamine (NH_2OH) oxidation, nitrifier denitrification, and heterotrophic denitrification (Kampschreur et al., 2009). The first two pathways occur inside the aerobic reactor mainly due to the ammonia oxidising bacteria (AOB) activity (White and Lehnert, 2016; Zhu-Barker et al., 2015). Further, from Period I to Period II, the gaseous N_2O–N concentration in each reactor increased (Fig. 4a and b). This result is likely attributed to the influence of the prolonged anaerobic conditions within the OSA reactor on the autotrophic biomass growth, as confirmed by the respirometry results (and consequently on the nitrification

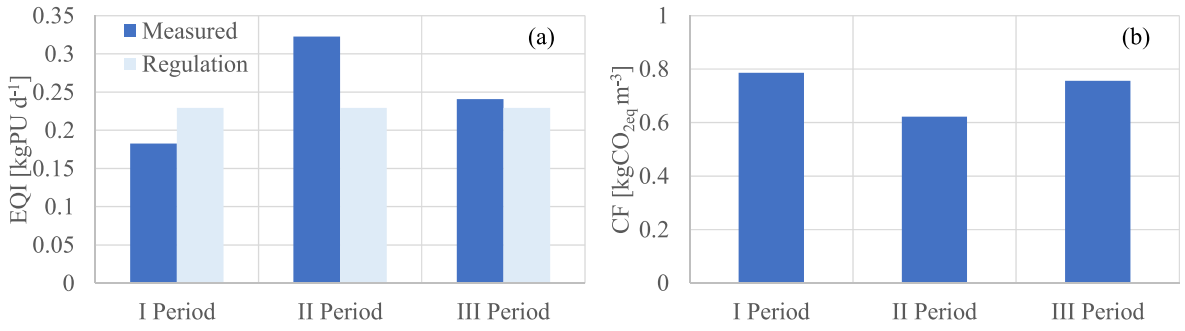

Fig. 5. EQI (a) and CF (b) for each Period.

process). From Period I to Period III, the average values of the gaseous N_2O–N concentration increased in all the reactors, especially in the OSA reactor, where denitrification influence could negatively affect GHG emissions. In terms of dissolved N_2O–N concentrations, results similar to those discussed for the gaseous form were obtained.

In terms of emission factors, the highest emission occurred during Period II. Indeed, 2.17%, 2.74% and 2.54% of the total influent nitrogen were emitted as N_2O during Periods I, II and III, respectively.

3.7. Carbon footprint and effluent quality

Fig. 5 shows the trend of both EQI and CF for each experimental Period. The measured EQI was compared with the EQI of legislation. This latter was calculated using effluent pollutant concentrations (TCOD, TN and P-PO_4), the limits imposed by the Italian Regulation (Legislative Decree No. 152/2006).

From data reported in Fig. 5a, it can be observed that except for Period I, the measured EQI was always higher than that obtained considering the Regulation limits. Specifically, during Period I, the EQI was equal to 0.18 kgPU d^{-1}, around 20% lower than that obtained considering the regulation limits (0.23 kgPU d^{-1}). During Periods II (0.32 kgPU d^{-1}) and III (0.24 kgPU d^{-1}), the calculated EQI was higher than that obtained considering the regulation limits (Fig. 5a). The increase of EQI during Periods II and III was mainly due to the discussed decrease in TN and PO_4 removal efficiencies.

By analysing Fig. 5b, it can be observed that the CF value varied during the three periods. The CF values were 0.78, 0.62, and 0.75 $kgCO_{2eq}$ m^{-3} during Period I, II, and III, respectively. The increase in CF during Period III was mainly related to the rise of indirect emissions due to the higher energy consumption than in the previous periods. Indeed, the energy consumption during Period I was 48.24 kWh d^{-1}. This value increased to 48.84 and 49.5 kWh d^{-1} during Periods II and III. The increase in energy consumption is due to the higher frequency of the pump recirculating the sludge from MBR to the OSA reactor. Compared to the others, the reduction of CF during Period II is due to the lower contribution due to the oxidation of the organic substance ($CO_{2,OrgOx}$) caused by the lower carbon consumption during denitrification.

4. Conclusions

This study showed that: i. the highest (88%) biological sludge reduction was obtained under the operation with IR of 100%, with heterotrophic observed yield coefficient of 0.15 gTSS/gCOD; ii. the sludge reduction was due to the cell lysis and endogenous metabolism; iii. with the increase of IR, a worsening in terms of membrane fouling (therefore operating costs) and greenhouse gas emissions occurred simultaneously. However, the CF was maintained almost equal to that obtained under the operation with an IR of 45%. Therefore, a trade-off between the advantages of reducing sludge production and the disadvantages of increasing membrane fouling and GHG emissions must be identified in the future. Further developments should be devoted to optimising the operational features of OSA-MBR systems, minimising excess sludge production, controlling fouling tendency, and decreasing GHG emissions.

CRediT authorship contribution statement

Paulo Marcelo Bosco Mofatto: Conceptualization, Data curation, Formal analysis, Funding acquisition, Investigation, Methodology, Resources. **Alida Cosenza:** Conceptualization, Data curation, Formal analysis, Investigation, Methodology, Resources, Validation, Writing – original draft, Writing – review & editing. **Daniele Di Trapani:** Conceptualization, Data curation, Formal analysis, Investigation, Methodology, Resources, Validation, Writing – original draft, Writing – review & editing. **Giorgio Mannina:** Conceptualization, Data curation, Formal analysis, Funding acquisition, Investigation, Methodology, Resources, Supervision, Validation, Writing – original draft, Writing – review & editing.

Declaration of competing interest

The authors declare that they have no known competing financial interests or personal relationships that could have appeared to influence the work reported in this paper.

Data availability

The data that has been used is confidential.

Acknowledgments

This work was funded by the project “Achieving wider uptake of water-smart solutions—WIDER UPTAKE” (grant agreement number: 869283) financed by the European Union’s Horizon 2020 Research and Innovation Programme, in which the last author of this paper, Giorgio Mannina, is the principal investigator for the University of Palermo. The Unipa project website can be found at: https://wideruptake.unipa.it/.

Appendix A. Supplementary data

Supplementary data to this article can be found online at https://doi.org/10.1016/j.jenvman.2024.120345.

References

APHA, 2012. Standard Methods for the Examination of Water and Wastewater. Standard Methods.

Boiocchi, R., Viotti, P., Lancione, D., Stracqualursi, N., Torretta, V., Ragazzi, M., Ionescu, G., Rada, E.C., 2023. A study on the carbon footprint contributions from a large wastewater treatment plant. Energy Rep. 9, 274–286.

Chen, W., Mo, j, Du, X., Zhang, Z., Zhang, W., 2019. Biomimetic dynamic membrane for aquatic dye removal. Biomimetic dynamic membrane for aquatic dye removal. Water Res. 151, 243–251. https://doi.org/10.1016/j.watres.2018.11.078.

Cheng, C., Geng, J., Zhou, Z., Yu, Q., Gao, R., Shi, Y., Wang, L., Ren, H., 2021. A novel anoxic/aerobic process coupled with a micro-aerobic/anaerobic side-stream reactor filled with packing carriers for in-situ sludge reduction. J. Clean. Prod. 311, 127192.
Chudoba, P., Morel, A., Capdeville, B., 1992. The case of both energetic uncoupling and metabolic selection of microorganisms in the OSA activated sludge system. Environ. Technol. 13 (8), 761–770.
Collivignarelli, M.C., Abbà, A., Miino, M.C., Caccamo, F.M., Argiolas, S., Bellazzi, S., Bertanza, G., 2021. Strong minimisation of biological sludge production and enhancement of phosphorus bioavailability with a thermophilic biological fluidised bed reactor. Process Saf. Environ. Protect. 155, 262–276.
Cosenza, A., Di Bella, G., Mannina, G., Torregrossa, M., 2013. The role of EPS in fouling and foaming phenomena for a membrane bioreactor. Bioresour. Technol. 147, 184–192.
Cosenza, A., Di Trapani, D., Bosco Mofatto, P.M., Mannina, G., 2023. Sewage sludge minimisation by OSA-MBR: a pilot plant experiment. Chemosphere 347, 140695. https://doi.org/10.1016/j.chemosphere.2023.140695.
Culaba, A.B., Mayol, A.P., San Juan, J.L.G., Ubando, A.T., Bandala, A.A., Concepcion, R. S., Alipio, M., Chen, W.-H., Show, P.L., Chang, J.-S., 2022. Design of biorefineries towards carbon neutrality: a critical review. Bioresour. Technol. 128256.
Di Bella, G., Di Trapani, D., Judd, S., 2018. Fouling mechanism elucidation in membrane bioreactors by bespoke physical cleaning. Separ. Purif. Technol. 199, 124–133.
Di Trapani, D., Di Bella, G., Mannina, G., Torregrossa, M., Viviani, G., 2014. Comparison between moving bed-membrane bioreactor (MB-MBR) and membrane bioreactor (MBR) systems: influence of wastewater salinity variation. Bioresour. Technol. 162, 60–69.
Etienne, P., Yu-Tung, L., 2012. Aerobic granular sludge technology for wastewater treatment. In: Etienne, P., Yu-Tung, L. (Eds.), Biological Sludge Minimisation and Biomaterials/Bioenergy Recovery Technolog^{ie}s, first ed. Wiley, New Jersey, USA.
Ferrentino, R., Langone, M., Andreottola, G., 2021. Sludge reduction by an anaerobic side-stream reactor process: a full-scale application. Environ. Challenges 2, 100016.
Ferrentino, R., Langone, M., Villa, R., Andreottola, G., 2018. Strict anaerobic side-stream reactor: effect of the sludge interchange ratio on sludge reduction in a biological nutrient removal process. Environ. Sci. Pollut. Res. 25, 1243–1256.
Fida, Z., Price, W.E., Pramanik, B.K., Dhar, B.R., Kumar, M., Jiang, G., Hai, F.I., 2021. Reduction of excess sludge production by membrane bioreactor coupled with anoxic side-stream reactors. J. Environ. Manag. 281, 111919.
IPCC 2022 - Intergovernmental Panel on Climate Change Sixth Assessment Report https://www.ipcc.ch/report/ar6/wg3/.
Kampschreur, M.J., Temmink, H., Kleerebezem, R., Jetten, M.S.M., van Loosdrecht, M.C. M., 2009. Nitrous oxide emission during wastewater treatment. Water Res. 43, 4093–4103.
Legislative Decree, 2006. N. 152 on Environmental Regulations, 3 April.
Liu, X., Iqbal, A., Huang, H., Zan, F., Chen, G., Wu, D., 2021. Life cycle assessment of deploying sludge minimisation with (sulfidogenic-) oxic-settling-anaerobic configurations in sewage-sludge management systems. Bioresour. Technol. 335, 125266.
Mannina, G., Cosenza, A., 2015. Quantifying sensitivity and uncertainty analysis of a new mathematical model for the evaluation of greenhouse gas emissions from membrane bioreactors. J. Membr. Sci. 475, 80–90.
Mannina, G., Gulhan, H., Ni, B.-J.,2022. Water reuse from wastewater treatment: The transition towards circular economy in the water sector. Bioresource Technology 363, 127951. https://doi.org/10.1016/j.biortech.2022.127951.
Mannina, G., Morici, C., Cosenza, A., Di Trapani, D., Ødegaard, H., 2016a. Greenhouse gases from sequential batch membrane bioreactors: a pilot plant case study. Biochem. Eng. J. 112, 114–122.
Mannina, G., Cosenza, A., Di Trapani, D., Laudicina, V.A., Morici, C., Ødegaard, H., 2016b. Nitrous oxide emissions in a membrane bioreactor treating saline wastewater contaminated by hydrocarbons. Bioresour. Technol. 219, 289–297. https://doi.org/10.1016/j.biortech.2016.07.124.
Mannina, G., Capodici, M., Cosenza, A., Cinà, P., Di Trapani, D., Puglia, A.M., Ekama, G. A., 2017. Bacterial community structure and removal performances in IFAS-MBRs: a pilot plant case study. J. Environ. Manag. 198, 122–131.
Mannina, G., Ekama, G.A., Capodici, M., Cosenza, A., Di Trapani, D., Ødegaard, H., van Loosdrecht, M.C.M., 2018. Influence of carbon to nitrogen ratio on nitrous oxide emission in an integrated fixed film activated sludge membrane BioReactor plant. J. Clean. Prod. 176, 1078–1090.
Mannina, G., Alduina, R., Badalucco, L., Barbara, L., Capri, F.C., Cosenza, A., Di Trapani, D., Gallo, G., Laudicina, V.A., Muscarella, S.M., Presti, D., 2021a. Water resource recovery facilities (Wrrfs): the case study of Palermo University (Italy). Water 13, 3413.
Mannina, G., Badalucco, L., Barbara, L., Cosenza, A., Di Trapani, D., Gallo, G., Laudicina, V.A., Marino, G., Muscarella, S.M., Presti, D., Helness, H., 2021b. Enhancing a transition to a circular economy in the water sector: the EU project WIDER UPTAKE. Water 13 (7), 946. https://doi.org/10.3390/w13070946.
Mannina, G., Cosenza, A., Di Trapani, D., Gulhan, H., Mineo, A., Bosco Mofatto, P.M., 2023a. Reduction of sewage sludge and N2O emissions by an Oxic Settling Anaerobic (OSA) process: the case study of Corleone (Italy) wastewater treatment plant. Sci. Total Environ. 906, 167793. https://doi.org/10.1016/j.scitotenv.2023.167793.
Mannina, G., Barbara, L., Cosenza, A., Wang, Z., 2023b. Treatment and disposal of sewage sludge from wastewater in a circular economy perspective. Curr. Dev. Biotechnol. Bioeng. 11–30. https://doi.org/10.1016/B978-0-323-99920-5.00011-1.
Metcalf, Eddy, 2015. Wastewater Engineering Treatment and Resource Recovery, fifth ed.
Morello, R., Di Capua, F., Pontoni, L., Papirio, S., Spasiano, D., Fratino, U., Pirozzi, F., Esposito, G., 2021. Microaerobic digestion of low-biodegradable sewage sludge: effect of air dosing in batch reactors. Sustainability 13 (17), 9869.
Romero-Pareja, P.M., Aragon-Cruz, C.A., Quiroga-Alonso, J.M., Coello-Oviedo, M.D., 2017. Incorporating the Oxic-Settling-Anaerobic (OSA) process into an anoxic–oxic system for sewage sludge reduction and nutrient removal. Environ. Prog. Sustain. Energy 37 (3), 1068–1074, 2017.
Semblante, G.U., Hai, F.I., Ngo, H.H., Guo, W., You, S.J., Price, W.E., Nghiem, L.D., 2014. Sludge cycling between aerobic, anoxic and anaerobic regimes to reduce sludge production during wastewater treatment: performance, mechanisms, and implications. Bioresour. Technol. 155, 395–409.
Semblante, G.U., Hai, F.I., Bustamante, H., Price, W.E., Nghiem, L.D., 2016. Effects of sludge retention time on oxic-settling-anoxic process performance: biosolids reduction and dewatering properties. Bioresour. Technol. 218, 1187–1194.
Tsuneda, S., Mikami, M., Kimochi, Y., Hirata, Y., 2005. Effect of salinity on nitrous oxide emission in the biological nitrogen removal process for industrial wastewater. J. Hazard Mater. 119, 93–98.
White, C.J., Lehnert, N., 2016. Is there a pathway for N_2O production from hydroxylamine oxidoreductase in ammonia-oxidising bacteria? Proc. Natl. Acad. Sci. USA 113, 14474–14476.
Zhang, M., Yao, J., Wang, X., Hong, Y., Chen, Y., 2019. The microbial community in filamentous bulking sludge with the ultra-low sludge loading and long sludge retention time in oxidation ditch. Sci. Rep. 9, 1–10.
Zhang, W., Jiang, F., 2019. Membrane fouling in aerobic granular sludge (AGS)-membrane bioreactor (MBR): effect of AGS size. Water Res. 157, 445–453. https://doi.org/10.1016/j.watres.2018.07.069.
Zhang, R., Mao, Y., Meng, L., 2021a. Excess sludge cell lysis by ultrasound combined with ozone. Sep. Purif. Technol. 276, 119359.
Zhang, W., Liang, W., Zhang, Z., Hao, T., 2021b. Aerobic granular sludge (AGS) scouring to mitigate membrane fouling: performance, hydrodynamic mechanism and contribution quantification model. Water Res. 188, 116518 https://doi.org/10.1016/j.watres.2020.116518.
Zhang, W., Liang, W., Zhang, Z., 2022. Dynamic scouring of multifunctional granular material enhances filtration performance in membrane bioreactor: mechanism and modeling. J. Membr. Sci. 663, 120979 https://doi.org/10.1016/j.memsci.2022.120979.
Zhu-Barker, X., Cavazos, A.R., Ostrom, N.E., Horwath, W.R., Glass, J.B., 2015. The importance of abiotic reactions for nitrous oxide production. Biogeochemistry 126, 251–267.